Random electric fields and impurity diffusion in δ layers

N. S. Averkiev and A. M. Monakhov
Ioffe Physical-Technical Institute, 194021 St-Petersburg, Russia

A. Shik
Energenius Centre for Advanced Nanotechnology, University of Toronto, Toronto, Canada M5S 3E3

P. M. Koenraad and J. H. Wolter
COBRA Inter-University, Eindhoven University of Technology, P. O. Box 513, NL-5600MB Eindhoven, The Netherlands

(Received 8 July 1999)

Impurity diffusion in the δ layer during the process of its growth has been considered. Experiments show that the spreading of the impurity profile has a complex dependence on the in-plane impurity concentration. We carried out the numerical simulation of the self-consistent diffusion problem for the impurities moving in their own random electric field and have shown that at some critical impurity concentration in δ layer the impurity distribution function perpendicular to the layer acquires a non-Gaussian character.

I. INTRODUCTION

The present state of molecular beam epitaxy allows one to fabricate semiconductor structures with an almost arbitrary profile of dopant concentration along the growth axis. One of the most important achievements in this respect is the so-called δ layer, i.e., structures with a planar distribution of impurity ions. In ideal δ layers all impurities are concentrated in one single monolayer but the direct measurements show[1,2] that in real structures ions can be distributed over several monolayers due to diffusion during the structure growth. This spreading of the impurity profile may change noticeably the energy spectrum and other electronic properties of δ layers,[3,4] The in-plane impurity distribution is also of a considerable importance. Randomly placed impurity ions create large fluctuations of local electric fields whereas the amplitude decreases in the presence of correlation in the ion positions. These factors influence the carrier mobility[5–7] and the optical spectra of doped samples.[8] Thus the calculation of the impurity distribution in δ layers represent an important physical problem.

To solve this problem, we must consider the diffusion of impurities during the process of layer growth. However, at the growth temperature (typically having the order of 700 K) impurities are ionized and electric forces caused by the above-mentioned fluctuations of local electric fields can strongly modify the diffusion processes and, hence, the resulting impurity distribution. The self-consistent diffusion problem for impurities moving in their own random electric fields will be considered in our paper. We will show that for a large enough impurity concentration, their distribution along the growth axis differs noticeably from the Gaussian distribution characterizing ordinary diffusion not influenced by electric fields.

II. ELECTRIC FIELD CALCULATION

In our approach we considered bare ion charges neglecting the effects of electron screening. This can be inadequate at large distances from the ions. However, the effects of electric field on the ion diffusion, which are of our primary interest, are noticeable only in the closest vicinity of the ions, at distances much less than the screening length at the growth temperature, which justifies our assumption. Nevertheless, it would be incorrect to say that we completely ignored the charge of free electrons. In fact, this charge is considered as a uniform background providing the total neutrality of the system.

The spatial distribution of the electric field created by an arbitrary system of ions can only be found numerically. For this purpose we use the procedure of Monte Carlo simulation. A similar procedure is also used for the calculation of diffusion and for this reason we discuss it in more detail.

We take a planar $L\times L$ lattice in the xy plane with a unit lattice constant. For a given density $n=N/L^2\ll 1$ we randomly distribute the point charges e over the lattice sites. For the drift out of the plain we are interested in the electric field component E_z in the sites of a similar lattice shifted by z_0 in the z direction. To exclude effects caused by the finite length of the lattice, we apply periodic boundary conditions assuming the pattern of ions to be repeated with the period L. As a result we find

$$E_z=\frac{2\pi e}{L^2}\left(-\mathrm{sign}(z)+\sum_m\sum_n e^{-k\sqrt{m^2+n^2}z_0}e^{ink\Delta x_i}e^{imk\Delta y_i}\right), \tag{1}$$

where Δx_i and Δy_i are the coordinates of ions related to the point where E_z is measured, $k=2\pi/L$.

For numerical purposes it is convenient to tabulate the E_z values given by Eq. (1), for different values of z_0. Due to the symmetry of the problem, it is enough to consider one eighth on the square containing only $(L+1)(L+3)/8$ rather than L^2 points (see in Fig. 1).

A typical result of the electric field distribution obtained by the numerical simulation is shown in Fig. 2 by the solid line.

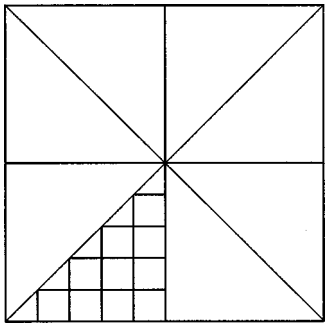

FIG. 1. The lattice site used in the field calculation.

It is interesting to compare this data with the analytical results which can be obtained for the noncorrelated distribution of ions in a similar way as the Holtsmark distribution of the gravitational field in a random system of stars.[9] Calculations given in Appendix A result in the following distribution function for E_z:

$$W(E_z)=\frac{1}{2\pi}\int_{-\infty}^{\infty}d\rho\,\exp[-i\rho E_z-nC(\rho)], \tag{2}$$

with

$$C(\rho)=\pi\int_{z_0^2}^{\infty}dx\left[1-\exp\left(i\rho\frac{ez_0}{x^{3/2}}\right)\right].$$

This function is shown by the dashed line in Fig. 2. A good correlation with the numerical results is seen, with an exception at the very small E_z where numerical simulation fails due to a limited size L of the lattice.

Far from the impurity layer, for $nz_0^2\gg 1$, the distribution function Eq. (2) is well described by the Gaussian distribution with the mean value $2\pi en$:

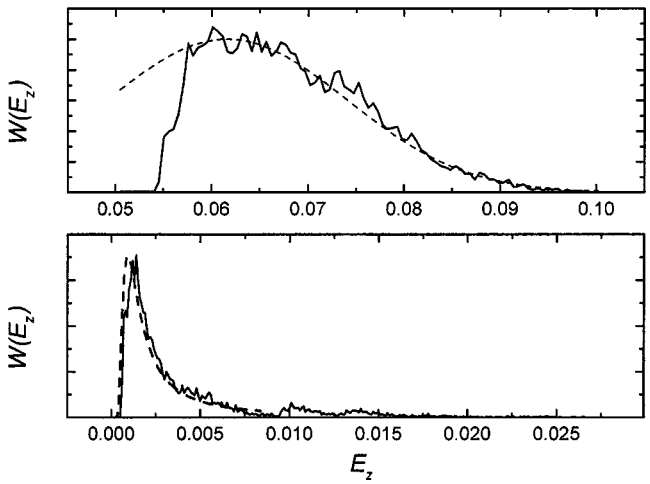

FIG. 2. Electric field distribution near the δ layer at different distances from it. The upper plot is drawn for $z=20$ lattice constants, the lower one for $z=0.1$. Solid lines show the results of the numerical simulation for 100 particles in a square with 100×100 lattice sites; dashed lines show the analytical results [Eqs. (3) and (4)].

$$W(E_z)=\frac{z_0}{\pi e\sqrt{n}}\exp\left[-\frac{z_0^2(E_z-2\pi en)^2}{\pi e^2 n}\right]. \tag{3}$$

At small distances, $nz_0^2\ll 1$, Eq. (2) can be written as

$$W(E_z)=\frac{1}{\pi E_z}\int_0^{\infty}\cos(t-\sqrt{3}\xi t^{2/3})\exp(-\xi t^{2/3})dt, \tag{4}$$

$$\xi=\frac{4\pi}{3}n\left(\frac{e}{E_z z_0^2}\right)^{2/3}.$$

For $\xi\ll 1$, that is for strong electric fields,

$$W(E_z)\cong\frac{n(ez_0)^{2/3}}{E_z^{5/3}}. \tag{5}$$

This asymptotic formula has a simple physical explanation. For small z_0, the high-field tail of the distribution function is caused by an ion nearest to the point $(0,0,z_0)$. For $nz_0^2\ll 1$ the probability for another ion to have similar r is negligible. In other words, the high-field tail $W(E_z)dE_z$ is determined by the probability that a single ion is found in the interval between r_E and r_E+dr where $E_z=ez_0(r_E^2+z_0^2)^{-3/2}$. This probability is proportional to $nr_E dr$ which results in Eq. (5).

The distribution function at small distances, Eq. (4), has some unusual properties. The average electric field $\overline{E_z}=\int dE_z E_z W(E_z)=2\pi en$—a common result for homogeneously charged layer, whereas the maximum of $W(E_z)$ lies at considerably lower fields. It is connected with a strong asymmetry of $W(E_z)$ and its slow decrease at large E_z [see Eq. (5)]. Such character of the distribution function reflects the presence of strong fluctuations of electric field in the direct vicinity of the impurity layer. As will be shown in the next section, these fluctuations may influence noticeably the diffusion process of δ layer.

III. FIELD-INDUCED IMPURITY DIFFUSION

A. General description

The exact profile of a δ layer is determined by the ion motion during epitaxy at growth temperature. There are many possible mechanisms of impurity motion in the crystal lattice which complicates dramatically the formulation of a quantitative model. In our work, we do not try to reach an exact quantitative correspondence between theory and experiment. We only want to demonstrate qualitatively how the unusual distribution of the electric field in real systems can reveal itself in impurity diffusion. That is why we restrict ourselves to a simple model that qualitatively describes the main properties of the drift/diffusion process.

We shall assume impurities to move between sites on a spatial lattice which can be both the substitional or interstitial sites of a real lattice. The probability of hopping to the nearest empty site in the time interval dt in the absence of external fields will be written as

$$W=A\cdot\exp\left(-\frac{U_{eff}}{kT}\right)dt, \tag{6}$$

where U_{eff} is the effective potential including both the hopping barrier between the initial and final site and a possible reconfiguration of neighboring atoms due to the transition.

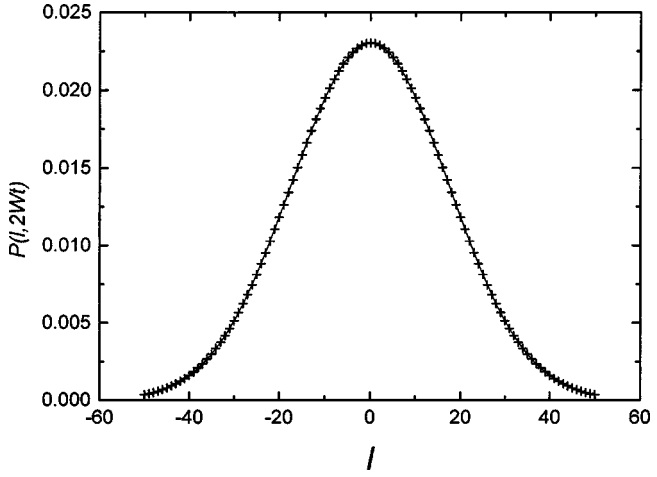

FIG. 3. Plot of the function (8) at $2Wt=300$ (crosses) and the respective Gaussian distribution (solid line).

To discuss the specific properties of impurity diffusion, let us consider in more detail the resulting distribution of impurities near the δ layer without electric field. According to Eq. (6), diffusion is a Poisson process. The probability to find a particle at the position l at the time t after this particle started from the origin is

$$\mathcal{P}(l,t)=\frac{1}{2\pi}\sum_n \frac{(2Wt)^n}{n!} \times \exp(-2Wt)\int_{-\pi}^{\pi}\cos^n\varphi\cdot\cos(l\varphi)d\varphi. \quad (7)$$

The first factor in Eq. (7) is the probability to make exactly n steps along any direction of z axis whereas the second factor is the well-known probability to reach the site l after n steps when there is an equal probability for moving right or left. This probability $\mathcal{P}(l,t)$ multiplied by the initial particle concentration, gives us the impurity distribution after the time t. Performing the summation in Eq. (7) before integration, we obtain

$$\mathcal{P}(l,t)=\exp(-2Wt)I_l(2Wt), \quad (8)$$

where $I_l(x)$ is the modified Bessel function. As can be seen from Fig. 3 for large values of Wt, $\mathcal{P}(l,t)$ as a function of l representing the z coordinate of a particle, coincides with a Gaussian distribution. Thus, when $t\gg 1/W$ our model in the absence of electric field describes normal diffusion.

The influence of Coulomb interaction between the charged impurities on the diffusion process can be taken into account by replacing Eq. (6) with

$$W_{ij}=A\cdot\exp\left(-\frac{U_{eff}-\Delta\varphi_{ij}/2}{kT}\right)dt. \quad (9)$$

Here $\Delta\varphi_{ij}$ is the difference in potential energy (determined by the electrostatic potential) between sites i and j. Equation (9) can be modified by introducing the effective time $d\tau=A\exp(-U_{eff}/kT)dt$ which depends on temperature. This is equivalent of introducing the effective dimensionless time $2Wt$ in Eq. (8). We concentrate our attention on the difference in the diffusion processes with and without electric field at the same temperature and will write the hopping probability between sites i and j as

$$W_{ij}=\exp\left(\frac{\Delta\varphi_{ij}}{2kT}\right)d\tau, \quad (10)$$

where the transition to normal diffusion corresponds to $\Delta\varphi_{ij}=0$. As a result, the hopping probability between different neighboring sites depends on $\Delta\varphi_{ij}$ and the effective equation for a large number of hopping events may differ drastically from the diffusion equation. Now the probabilities W_{ij} become dependent on the coordinates of all other particles which prevents us from obtaining a simple analytical expression. For this reason, we can only proceed by numerical simulation.

B. Numerical simulation of diffusion

The simulation procedure was organized in the following way. As in Sec. II, we take a $L\times L$ lattice and place $N=nL^2$ point charges on the lattice. Then we take an occupied ith site and with the help of formula Eqs. (B1) or (B5) given in Appendix B we calculate the potential differences $\Delta\varphi_{ij}$ between the given ith site and all empty neighboring sites, caused by all other charges. For this we can use the previously calculated array as it has been mentioned in Sec. II.

The electric potential, Eq. (B1) converges well outside the plane $z=0$. In the plane itself one should perform the Evald's transformation of the corresponding Fourier series given in more detail in Appendix B. This is not required for the calculation of E_z since at $z=0E_z=0$.

Next we calculated the probability of hopping to the corresponding empty site per unit time. The time interval $\Delta\tau$ is chosen such that the probability of a double hop in this time interval can be neglected. In accordance with the calculated probabilities, particles either moved or remained in place, after which the procedure was repeated.

Some results of our numerical simulations are presented in Fig. 4. The upper row shows the particle distribution at different times. The lower row in Fig. 4 shows the distribution at the same times τ where, instead of the self-consistent electric field, a homogeneous field of $\varphi=2\pi n|z|$ has been used in the calculations. In this case one can see that the distribution for $\tau=5$ is well approximated by a Gaussian distribution. Thus the non-Gaussian distribution observed at $\tau=5$ in the upper row is not due to the high electric field near the δ layer but due to fluctuations in the field strength. When the Coulomb interaction between the particles is completely neglected normal Gaussian distributions are obtained similar to those in the lower row in Fig. 4. The time needed to obtain distributions having the same width as in the lower part of Fig. 4 is however much longer as in the case that the electric field is included.

Calculations show that up to $n\simeq 0.04$ (which corresponds to the real impurity concentrations $\simeq 1.6\times 10^{13}$ cm^{-2}) the particle distribution after large enough time is well approximated by a Gaussian distribution. This means that up to these densities the process has a purely diffusional character and in the limit of large times obeys the standard diffusion equation.

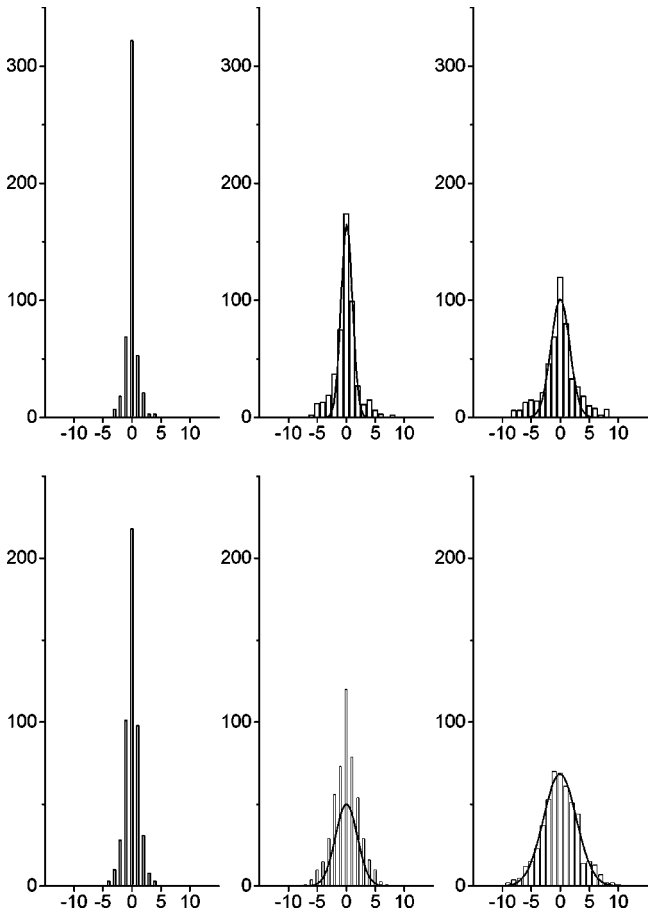

FIG. 4. Histograms of the impurity distribution near the δ layer (500 particles in a lattice of 100×100 unit cells). In the first column $\tau=1$, in the second $\tau=3$, and $\tau=5$ in the third one. The upper row shows the diffusion in the self-consistent electric field, whereas the lower one shows the diffusion in a constant electric field of $E_z=2\pi n$ containing no fluctuations. The solid lines show the Gaussian fits to the histograms.

At $n>0.04$ the distribution of particles at large enough time has an essentially non-Gaussian character. The distribution acquires well-developed shoulders. The explanation of this phenomenon lies in the fact that at small n strong field fluctuations are created only by tight clusters of a small number of particles. Such a cluster is rapidly expanded in the xy plane due to diffusion, and particles do not have enough time for moving far along the z axis until the fluctuation is dissolved.

The process changes its character when the probability to form a large enough cluster becomes noticeable. In this case the runaway probability in the xy plane decreases and the particles begin to move in z direction as well. Until the moment that strong field fluctuations are destroyed by diffusion, the particles escaping the plane will form shoulders in the density profile, which then will remain during diffusion in the mean electric field.

IV. COMPARISON WITH EXPERIMENT

It is interesting to compare the theoretical predictions given above with the results of experimental measurements. From a number of related experiments, we have chosen those

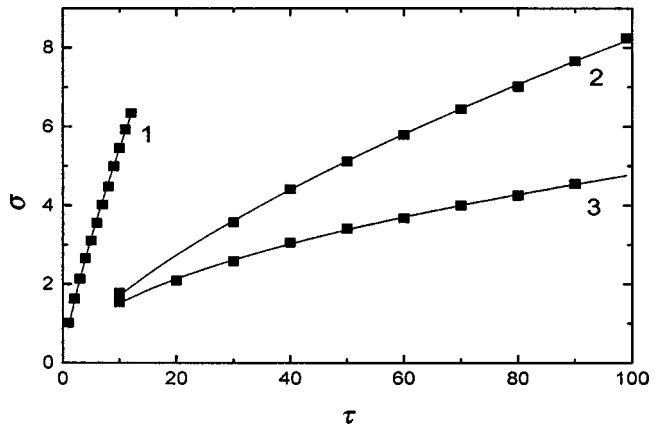

FIG. 5. Standard deviation as a function of τ for the different particle densities: 1 – $n_S=0.05$, 2 – $n_S=0.01$, and 3 – $n_S=0.001$.

where the impurity diffusion in Be δ-doped layers in GaAs was analyzed with cross-sectional STM.[2] By identifying single impurity atoms, this method allows to observe directly the δ-layer broadening and to draw histograms similar to those of Fig. 4. The drawback of the method is a lack in statistics. An X-STM histogram consists of no more than 60–70 doping atoms which is insufficient for direct comparison of the histograms obtained by STM and by numerical simulation.

The data of Ref. 2 show that for Be concentrations up to 10^{13} cm^{-2} no noticeable layer broadening is observed (this has been recently confirmed by experiments on Si-doped δ layers). At higher Be concentrations, a sharp δ layer broadening occurs (corresponding data for Si-doped layers are not available yet). The layer thickness was found to increase 10 times when the concentration increase from 10^{13} to 3×10^{13} cm^{-2}. The samples investigated in Ref. 2 contained a set of δ layers kept at the growth temperature for a different time which allowed us to investigate the time dependencies of the layer broadening. It was found that for the concentrations less than 10^{13} cm^{-2} this dependence is best approximated by the standard law $\sigma\sim\sqrt{\tau}$.

To compare the results of experiment and numerical simulation, we have analyzed the latter in the same way as the results of STM measurements. For a given concentration, the τ dependence of the standard deviation σ was plotted for the corresponding histograms. The dependence obtained was fitted to the curve

$$\sigma=a\tau^b. \tag{11}$$

For the normal diffusion, $b=1/2$ and a corresponds to the diffusion coefficient. Some of these $\sigma(\tau)$ dependencies (squares) are shown in Fig. 5 together with the fitting curves of Eq. (11) (solid lines).

The concentration dependence of fitting parameters a and b is shown in Fig. 6. As mentioned above, the non-Gaussian histogram broadening starts at the concentration close to 0.04 in our units which for GaAs corresponds to the ion density of order 1.3×10^{13} cm^{-2}. This value is in an excellent agreement with the STM data. Figure 6 demonstrates that b increases with concentration from almost 0.5 up to the value

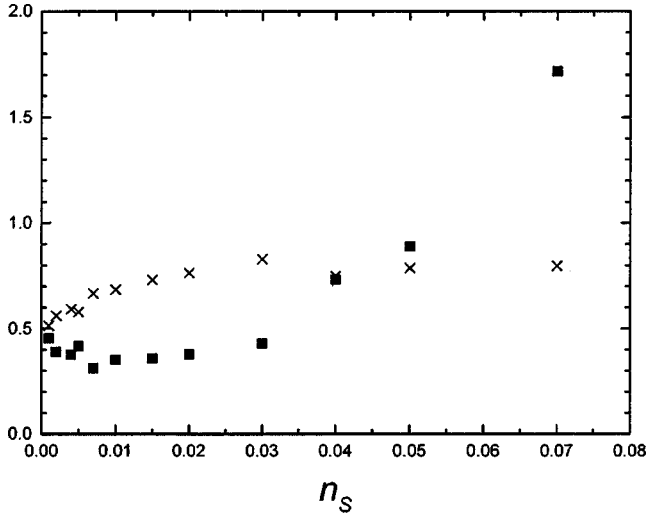

FIG. 6. The dependence of the parameters a (squares) and b (crosses) of the fitting curve (11) on the impurities concentration.

close to 0.8. This can be explained by the dominance of diffusion at low and of drift at higher concentrations.

The concentration dependence of a is much more interesting. This parameter varies slowly at the concentrations less than 0.04 and then demonstrates a steep growth. It is just the same concentration where non-Gaussian impurity distribution becomes noticeable. Thus the change in the diffusion/drift behavior at the critical concentration is revealed experimentally as a sharp increase in the observed ''diffusion coefficient.'' The layer thickness, as a function of concentration at fixed time and temperature, grows sharply in this region (see Fig. 5). The results are in a good agreement with experiment[2] both qualitatively and quantitatively.

V. CONCLUSION

To summarize, we have shown that at rather high impurity concentration in a δ layer, the impurity distribution function perpendicular to the layer acquires a non-Gaussian character because the process can no longer be described by a linear diffusion equation. The effect has a critical character, occurring above the critical dimensionless concentration ~ 0.04 and being almost invisible at lower concentrations. The above-mentioned critical behavior manifests itself experimentally as a step in the observed diffusion coefficient and, hence, in the δ layer thickness at the critical concentration.

ACKNOWLEDGMENTS

This work was partially supported by the program PhSSN 97-1039 and Nederlandse Organisatie voor Wetenschappelijk Onderzoek (NWO). One of the authors (A.S.) also thanks H. Ruda and Energenius Inc. for support.

APPENDIX A

Let us calculate the distribution function of the normal electric field component E_z. It is evident that at $z=0$, E_z is always zero but it appears as we move away from the impurity layer and when $z \gg 1/\sqrt{n}$ it has a constant value of $2\pi en$.

Let us consider a circle with the radius R containing N ions and find the probability $W_N(E_z)dE_z$ for the z component of electric field acting at an ion in the origin, to lie in the interval between E_z and E_z+dE_z. In the point $(0,0,z_0)$, the z component of electric field caused by an ion placed at $(x,y,0)$, is equal to $E_z = ez_0/(r^2+z_0^2)^{-3/2}$ with $r=\sqrt{x^2+y^2}$. Using this expression and applying Markoff's method described in Ref. 9 in more detail, we have

$$W_N(E_z) = \frac{1}{2\pi}\int_{-\infty}^{\infty} d\rho \exp(-i\rho E_z) A_N(\rho), \tag{A1}$$

where

$$A_N(\rho \mathbf{r}) = \prod_{i=1}^{N} \frac{1}{\pi R^2}\int_{|\mathbf{r}_i|=0}^{R} d^2\mathbf{r}_i \exp\left(i\rho \frac{ez_0}{(r_i^2+z_0^2)^{3/2}}\right). \tag{A2}$$

If we subsequently let R and N go to infinity while keeping the ion density n constant, $\lim_{R\to\infty}(3N/4\pi R^3)=n$, then $A_N(\rho)$ tends to

$$A(\rho) = \exp\left(-2\pi n \int_0^{\infty} r\, dr \left\{ 1-\exp\left[i\rho \frac{ez_0}{(r^2+z_0^2)^{3/2}}\right]\right\}\right), \tag{A3}$$

which eventually gives the final formula Eq. (2).

The distribution function for the in-plane electric field $\mathbf{E}_\parallel$ can be derived in a similar way:

$$W(E_\parallel) = \frac{1}{2\pi}\int_0^{\infty} d\rho\, \rho J_0(\rho E_\parallel)\exp(-\pi en\rho)$$

$$= \frac{en}{2E_\parallel^3}\frac{1}{[(\pi ne/E_\parallel)^2+1]^{3/2}}. \tag{A4}$$

APPENDIX B

To use periodic boundary conditions, one should calculate the potential in a point (x,y,z) created by a periodic two-dimensional rectangular (for simplicity, squared) lattice of point charges. For points outside the lattice plane $z=0$, the problem is easily solved by summation of the Fourier series

$$\varphi(x,y,z) = \frac{2\pi}{L^2}\left[-|z| + \sum_{m,n} \frac{\exp(-k\sqrt{m^2+n^2}|z| + imx + iny)}{k\sqrt{m^2+n^2}}\right]. \tag{B1}$$

This series converses well outside the $z=0$ plane. For $z=0$ the situation becomes more difficult and at x or y equal to zero, the series formally diverges. Similar problems are well known in the theory of lattice sums for ionic crystals. One of the possible tricks successfully used for their solution is the Evald's transformation of the initial series (see, e.g., Ref. 10) which will be used below with the account of specific features of our system.

To evaluate the formal sum

$$S=\sum_{n=-\infty}^{\infty}\sum_{m=-\infty}^{\infty}\frac{1}{\sqrt{(x-nL)^2+(y-mL)^2+z^2}}, \quad \text{(B2)}$$

we use the relation $1/|z|=(2/\sqrt{\pi})\int_0^\infty \exp(-z^2\rho^2)d\rho$, which gives us

$$S=\sum_{m,n}\frac{2}{\sqrt{\pi}}\int_0^\infty \exp\{-[(x-nL)^2+(y-mL)^2+z^2]\rho^2\}d\rho. \quad \text{(B3)}$$

The integrand in Eq. (B3) is a periodic function in the xy plane which could be expanded in a Fourier series by analogy with[10]

$$S=\frac{2\pi}{L^2}\sum_{m,n}\int_0^G\frac{1}{\rho^2}\exp\left[-\frac{k^2(m^2+n^2)}{4\rho^2}-z^2\rho^2+iknx+ikmy\right]d\rho+\frac{2}{\sqrt{\pi}}\sum_{m,n}\int_G^\infty \exp\{-[(x-nL)^2+(y-mL)^2+z^2]\rho^2\}d\rho. \quad \text{(B4)}$$

Here $k=2\pi/L$ and the constant G are chosen empirically to provide fast convergence of the series. Equation (B4) at $G\to\infty$ transforms into Eq. (B1). All integrals in Eq. (B4) are expressed in terms of the complementary error function $\mathrm{erfc}(x)=(1/\sqrt{\pi})\int_x^\infty \exp(-t^2)dt$ and, eventually,

$$S=\frac{\pi}{kL^2}\sum_{n=-\infty}^{\infty}\sum_{m=-\infty}^{\infty}\frac{\exp(iknx+ikmy)}{\sqrt{m^2+n^2}}\times\left[\exp(k\sqrt{m^2+n^2}z)\,\mathrm{erfc}\left(\frac{k\sqrt{m^2+n^2}}{2G}+zG\right)+\exp(-k\sqrt{m^2+n^2}z)\,\mathrm{erfc}\left(\frac{k\sqrt{m^2+n^2}}{2G}-zG\right)\right]+\sum_{n=-\infty}^{\infty}\sum_{m=-\infty}^{\infty}\frac{\mathrm{erfc}(\sqrt{z^2+(x+nL)^2+(y+mL)^2}\cdot G)}{\sqrt{z^2+(x+nL)^2+(y+mL)^2}}. \quad \text{(B5)}$$

[1] E. F. Schubert, in *Delta-doping of Semiconductors*, edited by E. F. Schubert (Cambridge University Press, Cambridge, England, 1996), pp. 224 and 238.

[2] M. B. Johnson, P. M. Koenraad, W. C. van der Vleuten, H. W. M. Salemink, and J. H. Wolter, Phys. Rev. Lett. **75**, 1606 (1995).

[3] A. Zrenner, F. Koch, and K. Ploog, Surf. Sci. **196**, 671 (1988).

[4] P. M. Koenraad, F. A. P. Blom, C. J. G. M. Langerak, M. R. Leys, J. A. A. J. Perenboom, J. Singleton, S. J. R. M. Spermon, W. C. van der Vleuten, A. P. J. Voncken, and J. H. Wolter, Semicond. Sci. Technol. **5**, 861 (1990).

[5] A. F. J. Levi, S. L. McCall, and P. M. Platzman, Appl. Phys. Lett. **54**, 940 (1989).

[6] O. Mezrin and A. Shik, Superlattices Microstruct. **10**, 107 (1991).

[7] J. M. Shi, A. F. W. van de Stadt, F. M. Peeters, J. T. Devreese, and J. H. Wolter, Phys. Rev. B **55**, 13 093 (1997).

[8] B. I. Shklovskii and A. L. Efros, *Electronic Properties of Doped Semiconductors* (Springer-Verlag, Berlin, 1986).

[9] S. Chandrasekhar, Rev. Mod. Phys. **15**, 1 (1943).

[10] J. M. Ziman, *Principles of the Theory of Solids* (Cambridge University Press, Cambridge, England, 1964).